

## 1. Cosmochronology

A radioactive decay can in principle yield a very precise age dating technique for a specific star if the lifetime of the decaying isotope is known (that is usually well known from lab measurements), if the initial abundance of the decaying isotope is known, and if the current isotopic abundance, or the abundance of the product of the decay (sometimes called the “daughter”), can be measured. After all, the abundance of a decaying radioactive isotope is an negative exponential,  $N_r(t) = N_r(0) \exp(-t/\tau_r)$ .

One looks for an unstable isotope of an element whose production is well understood, one with a suitable lifetime (preferably at least 1 Gyr, ideally a few Gyr, but not more than 5 Gyr, otherwise it doesn’t decay much even over the age of the universe). Unless one is dealing with meteorites, where isotopic abundances can be measured in the lab, the isotope must have detectable spectral features in a suitable region of the stellar spectrum. Again important in the case of stars, where elemental abundances can be measured, but almost all isotopic abundances cannot, the element involved must have no stable isotope which has an abundance larger than the radioactive isotope. Otherwise it is difficult to measure any change in the elemental abundance.

The isotopes identified as most suitable for this purpose are all heavy  $r$ -process nuclei. These elements can only be made by neutron capture with Fe-peak seeds. They all lie beyond the last stable elements, lead and bismuth, and cannot be reached via the  $s$ -process of neutron capture. Thus their production mechanism is understood, and it is also understood that they decay to lead or bismuth.

The isotopes are:  $^{187}\text{Re}$  (half life  $4.5 \times 10^{10}$  yr,  $^{232}\text{Th}$ , half life  $1.4 \times 10^{10}$  yr, and two isotopes of uranium,  $^{235}\text{U}$  with a half life of  $7.0 \times 10^8$  yr and  $^{238}\text{U}$ , with a half life of  $4.5 \times 10^9$  yr. After about a Gyr, one can ignore the lighter U isotope and assume all  $^{235}\text{U}$  already decayed to lead.

Since one needs to know the initial abundances, and stars have different initial metallicities, the technique used is to compare the abundance ratios of the unstable isotope (element) to either another unstable isotope or to a stable one. The ratios most often used are Re/Os, Th/Eu, and Th/U. Eu has two stable isotopes; both are produced almost exclusively through the  $r$ -process of neutron capture.

If the goal is a determination of the age of the galaxy, then determining the age of the oldest galactic stars puts a lower limit on the age of the universe. For this purpose, such techniques can best be applied to extremely metal-poor halo stars enriched in  $r$ -process elements.

In practice, as distinct from in theory, there are many problems with with the application of this technique. The major concerns are listed below:

- (1) Uranium is VERY HARD to detect in stars. U II has a few lines but they are all very weak and blended. The first detection of uranium in any star was in 2001 (Cayrel et al, 2001, Nature, 409, 691). Uranium has only been detected in perhaps three metal-poor stars. Molecular bands of CH and CN in the spectra of higher metal abundance stars blends the spectrum in the region of the U II line at 3859 Å too much to permit a detection iof the very weak and blended U II line even the very accurately observed solar spectrum.
- (2) To date, the  $^{232}\text{Th}/^{151,153}\text{Eu}$  ratio currently provides the most common decay clock used for stars. But to use this requires assuming that the predictions for the initial  $r$ -process abundance distribution are very accurate and the  $r$ -process pattern over the mass range 130 to 238 is identical for all sites and for all stars.
- (3) Th/Eu is not good as the two elements are too far apart in atomic weight (atomic number 63 versus 93). This means there is lots of room for our understanding of  $r$ -process production to go astray. When predicting the initial production ratios, the uncertainty

is generally smaller when the two elements are as close in mass number as possible. Hf (hafnium) may be better than Eu, it is somewhat heavier (atomic number 72 instead of 63 for Eu), but is harder to detect.

(4) The usual lines for Th are from neutral thorium. They too are weak lines, hard to measure with accuracy, but not as impossible as those of uranium. But the europium lines are from singly ionized europium. It would be better to have both elements be detected from neutral lines, or both from singly ionized lines. Mixing the states of ionization means a stronger dependence on the accuracy of the model atmospheres and detailed abundance analyses.

(5) All of this relies on an accurate and detailed analysis of  $r$ -process neutron capture reaction networks. But there are still uncertainties in the theory, which involves neutron capture,  $\beta$ -decay, and fission properties of unstable isotopes of heavy elements far from the valley of stability. A major uncertainty lies in the adopted nuclear mass formula. Another is what happens to the extremely heavy unstable isotopes formed, those even heavier than uranium? The usual assumption is that they undergo spontaneous fission completely rather than decaying to lead or bismuth, and make no contribution to the mass range of importance here. Filling in those deficiencies requires better abundance determinations for the stable elements in the lead peak, which tend to have no detectable lines at optical wavelength, and only a few in the UV range that can be reached by HST+STIS. Laboratory experiments on the heavy unstable isotopes in this regime of atomic mass are also necessary. Recall that the final  $r$ -process production over the isotopes and elements depends on the initial metallicity as seed nuclei are required and also on the neutron flux as a function of time during the  $r$ -process event. Is the latter always the same?

(6) We still lack a self-consistent model that can produce the conditions for  $r$ -process nucleosynthesis; although core collapse SN are the favored candidate, neutron star mergers

may also be important sources. The identification with massive star environments is crucial as it implies that the nuclear chronometer began to run early in Galactic history.

(7) Are the  $r$ -process sites diverse ? Sometimes, but rarely, the Th/Eu age dating appears to fail and to give spurious results. There are two specific cases of weird ratios for Th/Eu known. The first is HD221170, in which Yushchenko, Gopka, Goriely et al (2005, A&A, 430, 255) detected 43 elements. The second is CS31082-001, analyzed by Hill et al (2002, A&A, 387, 560). These two stars have Th/Eu about a factor of 2.5 larger than in the normal old age dated very metal-poor stars, sometimes called the actinide “boost”, which suggests that the  $r$ -process *not* is not universal, and we do not understand this at all.

Having listed the problems, one must note from the appended table that at least we are getting the right ballpark for the age of the older stars in the galaxy, close to that from CDM cosmological models, the CMB,  $H_0$ , etc. But we are far from a precision measurement, where precision means  $\pm 10\%$ .

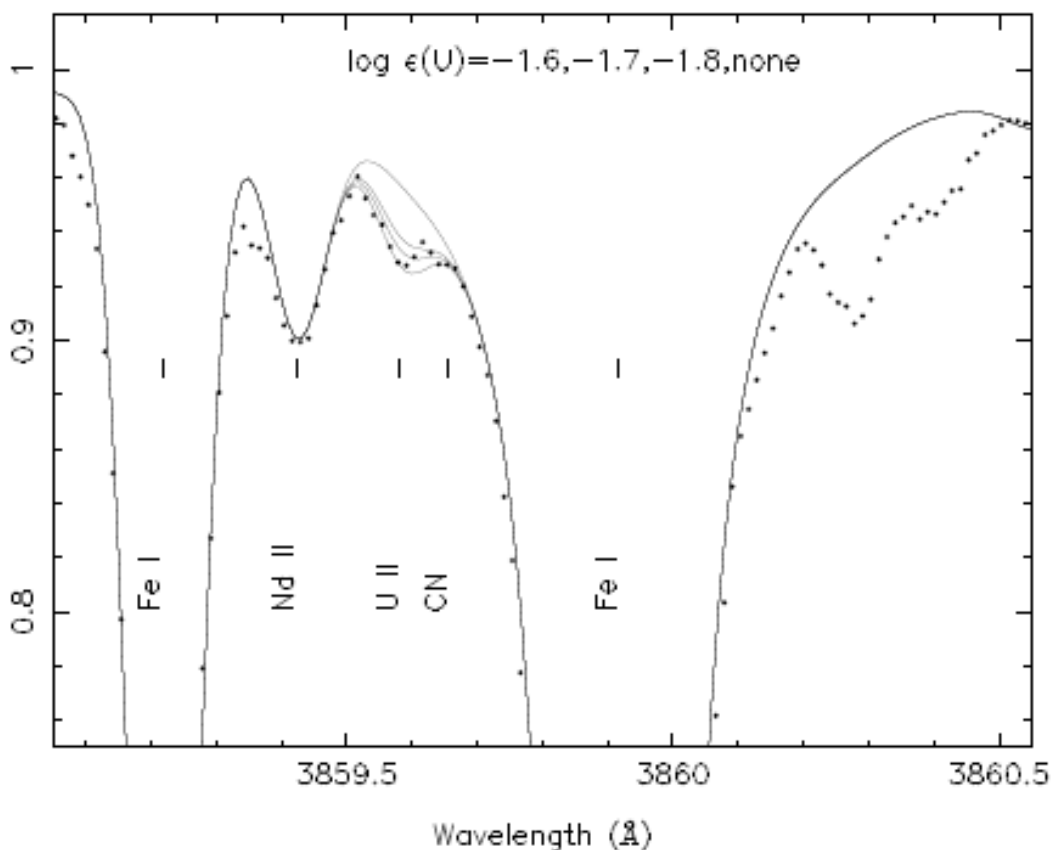


Figure 1: The spectrum of CS31082-001 around the U II line at 385.959 nm. The synthetic spectra (solid lines) were computed with the stellar atmospheric parameters given in the text, and for the three abundances indicated, adopting an oscillator strength  $f = 0.053$  for the line (ref.13). The observed spectrum (data points) was obtained in four hours for a total S/N ratio of 300.

Fig. 1.— The first stellar detection of uranium was claimed by Cayrel et al (2001). They detected one U II line at 3859.6 Å. Note the extensive blending and requirement for very high SNR spectra, a very complete line list, etc to get a U abundance from this weak, blended, crowded line. Claiming a detection of U on the basis of this single line in this star requires an act of faith beyond my ability to believe. (Fig. 1 of Cayrel et al, 2001)

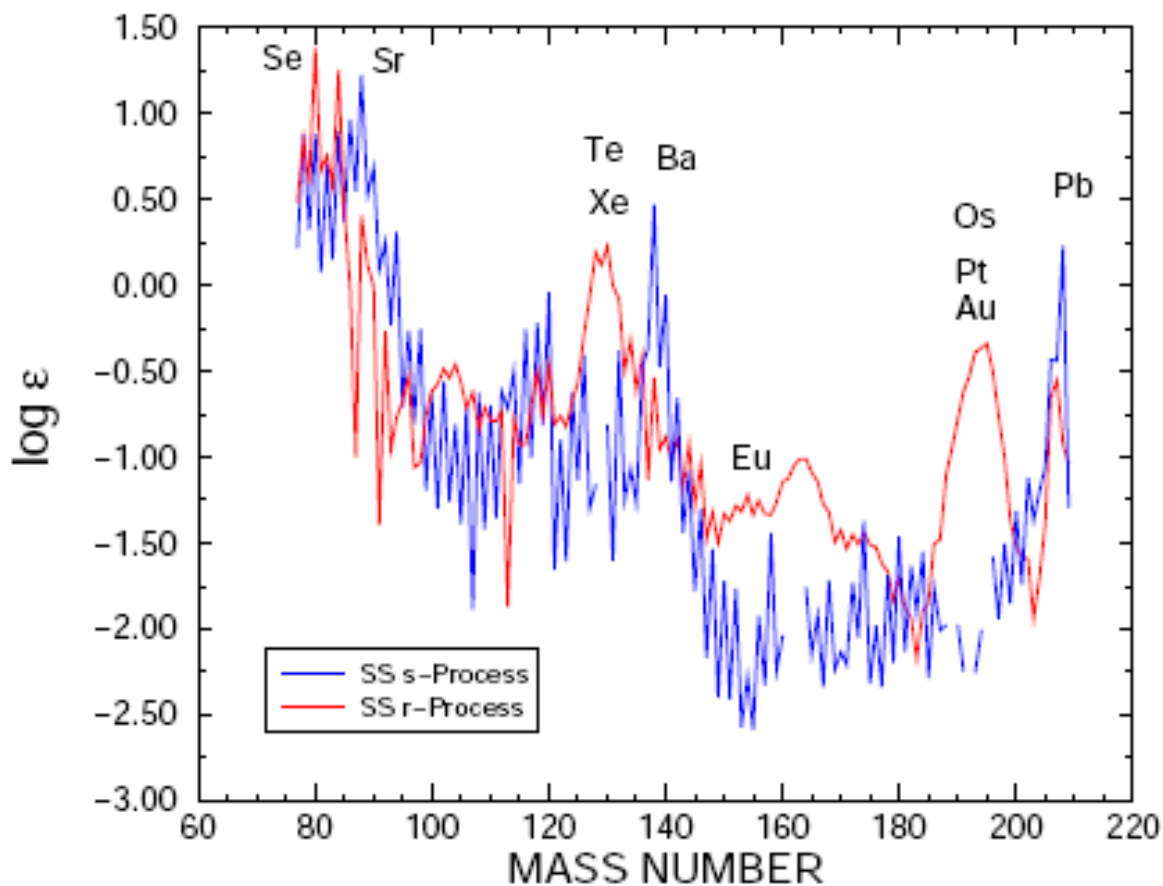


Fig. 1.— The *s*-process and *r*-process abundances in solar system matter, based upon the work by Käppeler *et al.* (1989). Note the distinctive *s*-process signatures at masses  $A \approx 88$ , 138, and 208 and the corresponding *r*-process signatures at  $A \approx 130$  and 195, all attributable to closed shell effects on neutron capture cross sections. It is the *r*-process pattern thus extracted from solar system abundances that can be compared with the observed heavy element patterns in extremely metal-deficient stars. The total solar system abundances for the heavy elements are those compiled by Anders and Grevesse (1989).

Fig. 2.— Solar system *r* vs *s* abundances beginning beyond the Fe-peak. (Fig. 1 of Truran, Cowan, Pilachowski & Sneden, 2002, PASP, 114, 1293)

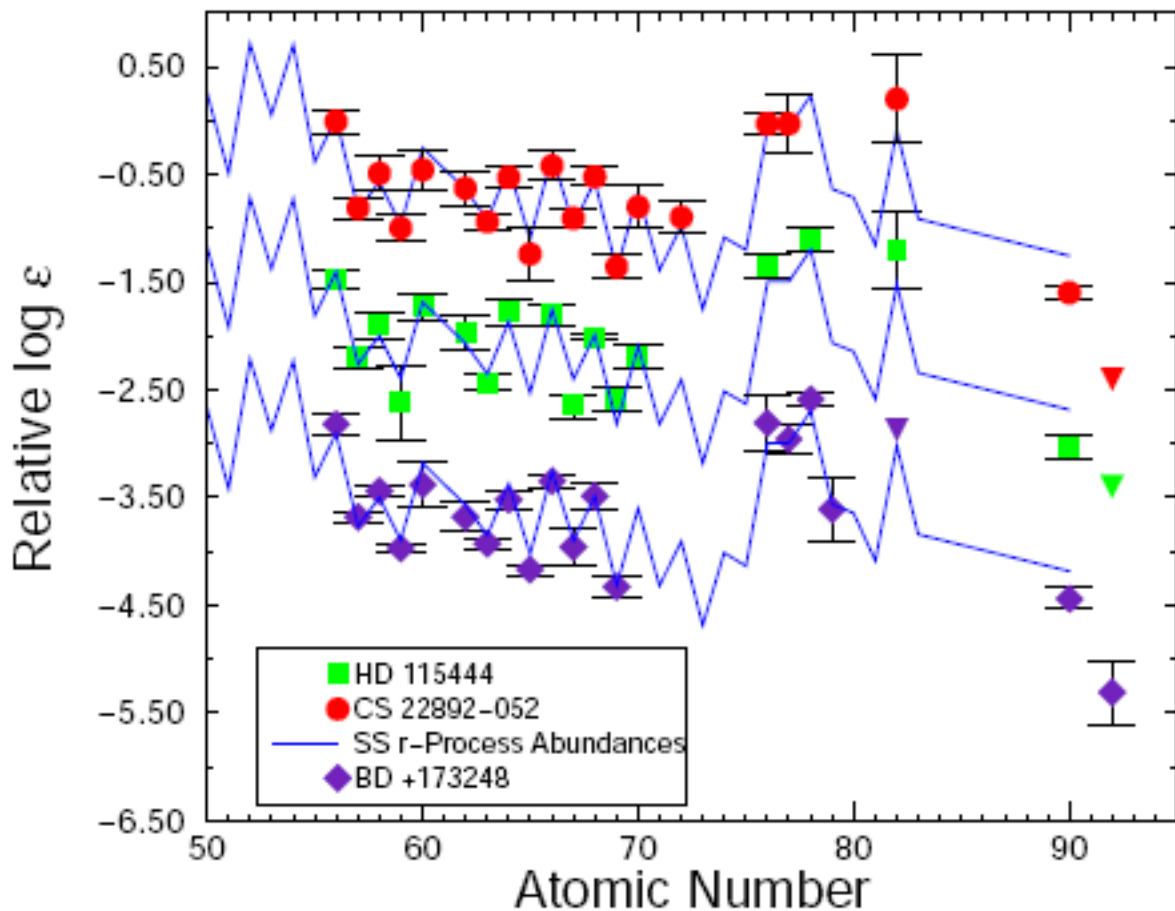


Fig. 3.— The heavy element abundance patterns for the three stars CS 22892-052, HD 155444 and BD +17<sup>o</sup>3248 are compared with the scaled solar system  $r$ -process abundance distribution (solid line). (see Sneden *et al.* 2000; Westin *et al.* 2000; Cowan *et al.* 2002) Upper limits are indicated by inverted triangles.

Fig. 3.— The heavy element abundances for three metal-poor  $r$ -enriched stars are compared to the scaled solar abundances beginning beyond the Fe-peak. This data provides a demonstration that the  $r$ -process production is universal, at least from the Ba peak to the heaviest elements. (Fig. 3 of Truran, Cowan, Pilachowski & Sneden, 2002)

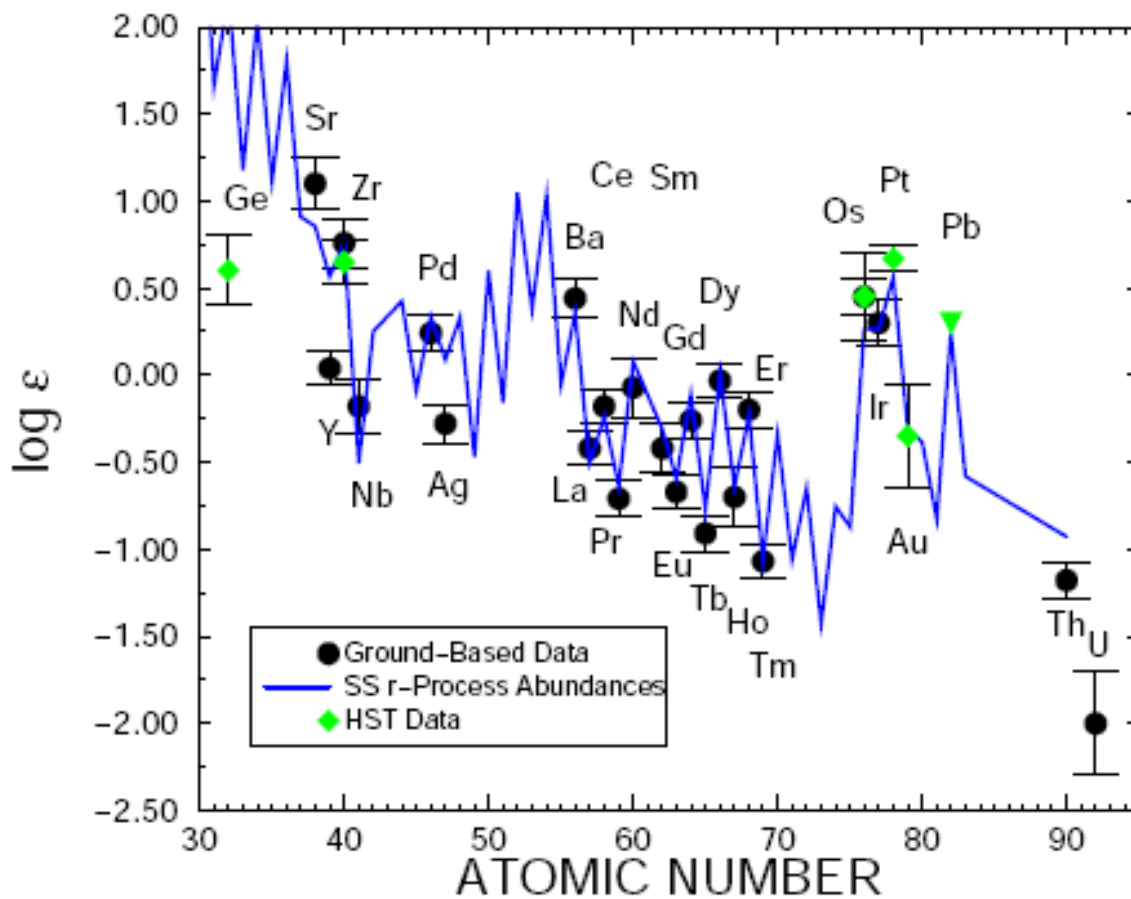


Fig. 4.— Neutron capture elements in the halo star BD +17°3248 (Cowan *et al.* 2002), obtained from ground based and HST observations, are compared to a scaled solar system  $r$ -process abundance curve. The upper limit on the lead abundance is denoted by an inverted triangle. Note also the thorium and uranium detections.

Fig. 4.— Note the apparent depletion of Th and U compared to the scaled solar distribution. (Fig. 4 of Truran, Cowan, Pilachowski & Sneden, 2002)



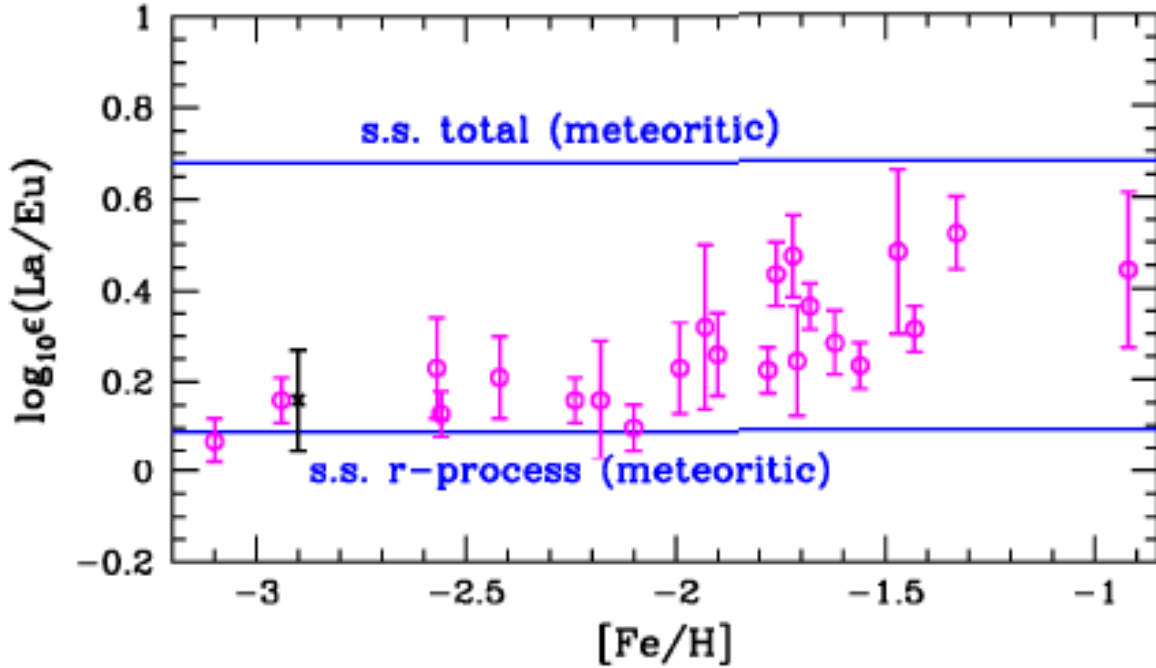


Fig. 8.— Ratio of La to Eu abundances in a few representative stars (open circles) over most of the Galactic halo metallicity range from Simmerer et al. (2002). The La abundances have been derived using new La II laboratory values from (Lawler *et al.* 2001). The data point indicated by an x is from Cayrel et al. (2001).

Fig. 5.— La represents an element whose production is dominated by the *s*-process of neutron capture; Eu is *r*-process dominated. The rise as metallicity  $[\text{Fe}/\text{H}]$  increases from *r*-process dominated to an increasing contribution from the slow neutron capture process. (Fig. 8 of Truran, Cowan, Pilachowski & Sneden, 2003)

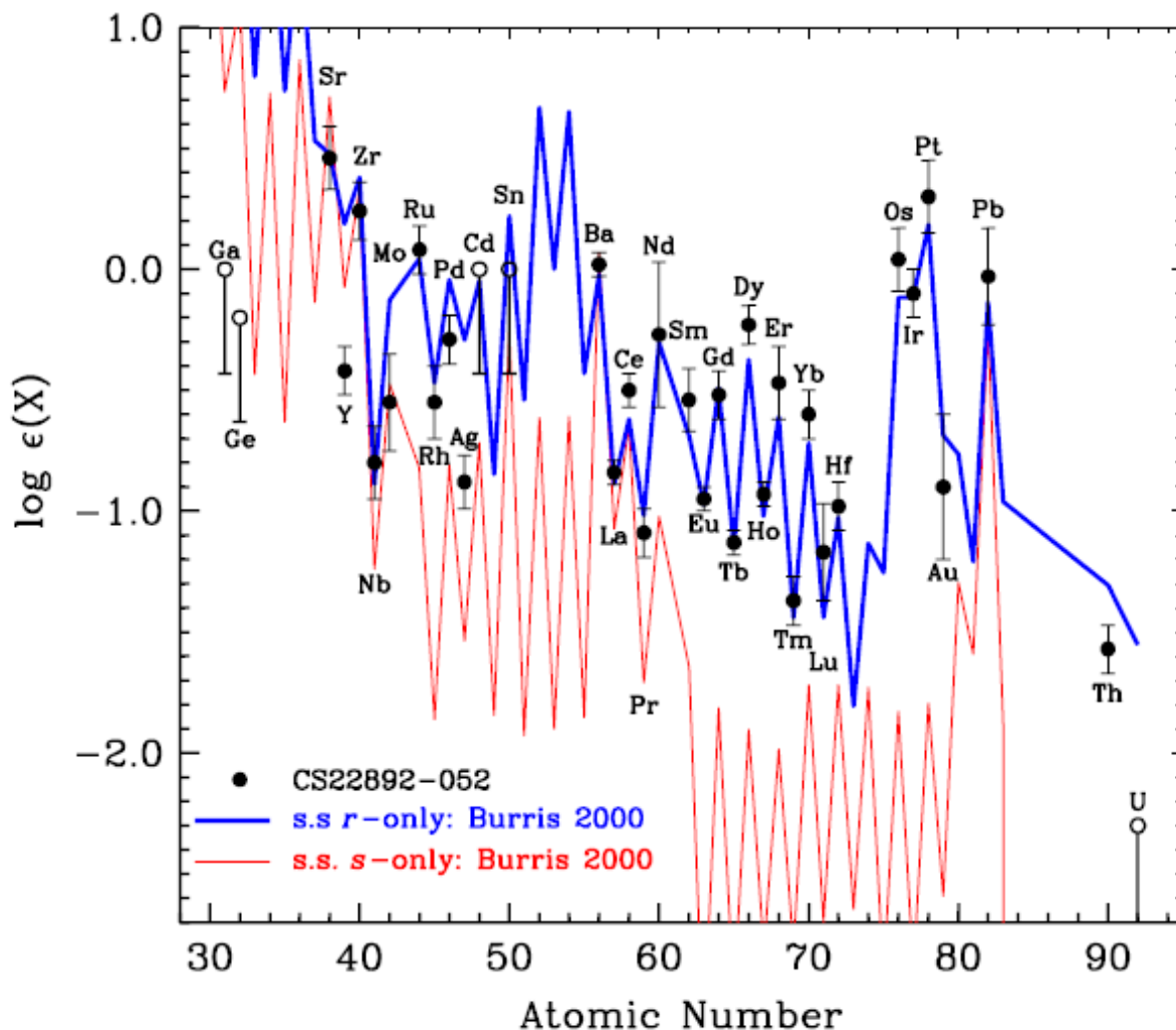


Fig. 6.— Observed  $n$ -capture abundances in CS 22892-052 and two scaled solar-system abundance distributions (Burriss et al. 2000). Detected elements are shown as solid circles with complete error bars, and upper limits are denoted with open circles with only the lower half of an arbitrary-length error bar. The solar-system  $r$ -process abundance set (solid line) is vertically scaled by a single additive constant to match the observed Eu abundance, while the  $s$ -process set (dashed line) is scaled to match the observed Ba abundance.

Fig. 6.— The neutron capture elements in the metal-poor  $r$ -process enhanced star CS 22892–052 compared to scaled solar system  $r$  and  $s$  abundances beginning beyond the Fe-peak. Abundances, or upper limits, for 57 elements have been determined for this star by Sneden, Cowan, Lawler, et al (2003). This is Fig. 6 of their paper.

Thorium/Europium Ages for Individual Stars

Object	[Fe/H]	$\log \epsilon_{Th}$	$\log \epsilon_{Eu}$	$\Delta$	(Th/Eu)	$\tau_*$
CS22892-052	-3.1	-1.57	-0.91	-0.66	0.22	16.8
HD 115444	-3.0	-2.23	-1.63	-0.60	0.25	14.4
HD 115444	-3.0	-2.21	-1.66	-0.55	0.28	12.1
HD 186478	-2.6	-2.25	-1.55	-0.70	0.20	18.9
HD 108577	-2.4	-1.99	-1.48	-0.51	0.31	10.1
M92 VII-18	-2.3	-1.94	-1.45	-0.49	0.32	9.4
BD +8 2856	-2.1	-1.66	-1.66	-1.16	0.32	9.4
K341 (M15)	-2.4	-1.47	-0.88	-0.59	0.25	14.4
K462 (M15)	-2.4	-1.26	-0.61	-0.65	0.22	16.8
CS31082-001	-3.0	-0.96	-0.70	-0.26	0.55	-

References: (1) Sneden *et al.* 2000a; (2) Westin *et al.* 2000; (3) Johnson & Bolte 2001; (4) Sneden *et al.* 2000b; Hill *et al.* 2001.

Fig. 7.— A list of stars with Th/Eu ages, current as of 2001. (Table 1 of Truran, Burles, Cowan & Sneden, 2002, conference proceedings, astro-ph/0109526)

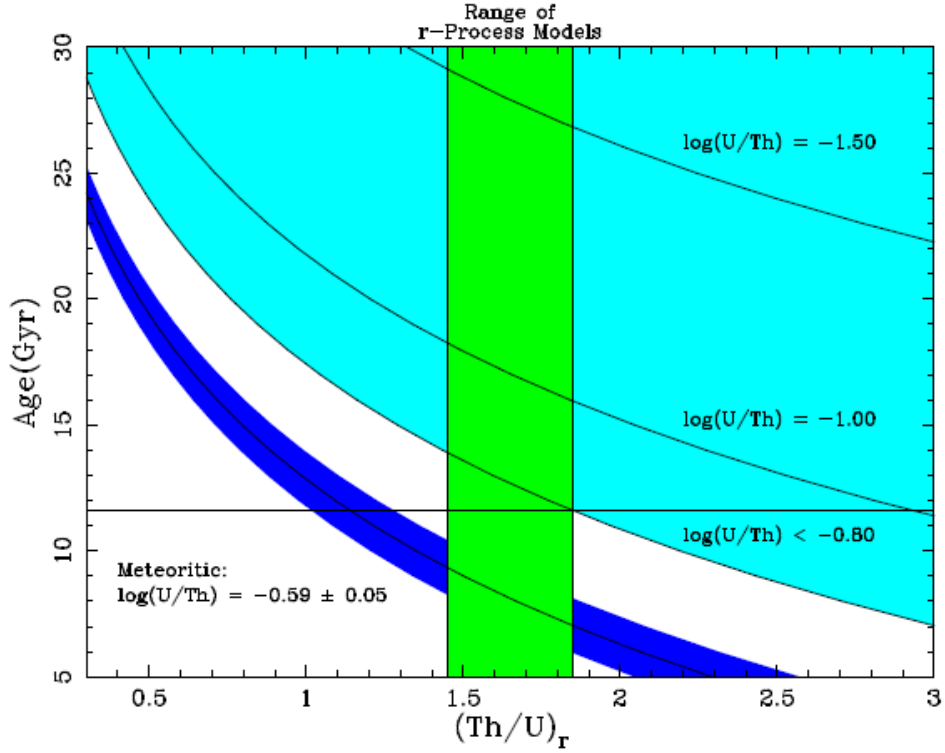


Figure 2. Stellar ages as a function of the Th/U ratio. Shown is the exponential dependence of the observed Th/U abundance on the age of the system. We assume that  $^{238}\text{U}$  dominates  $^{235}\text{U}$ , and therefore only show ages greater than 5 Gyrs. Lines of constant  $\log U/\text{Th}$  ratios are shown in the plane of Age vs.  $^{232}\text{Th}/^{238}\text{U}$  seed ratio. An upper limit on U/Th excludes the lower left half of the plane. A measurement of U/Th is restricted to a narrow band as is the case with meteoritic observations (Anders & Grevesse 1989).

Fig. 8.— Using upper limits to U/Th to set a lower limit on age. A precise age can be determined only if a uranium abundance can be measured for a star, which is extremely difficult. The X-axis is the ratio of Th/U at the source right after the  $r$ -process ends. The green vertical band indicates the range due to uncertainties in the nucleosynthesis and the resulting initial Th/U ratio for the  $r$ -process. (Fig. 2 of Truran, Burles, Cowan & Sneden, 2002, conference proceedings, astro-ph/0109526)

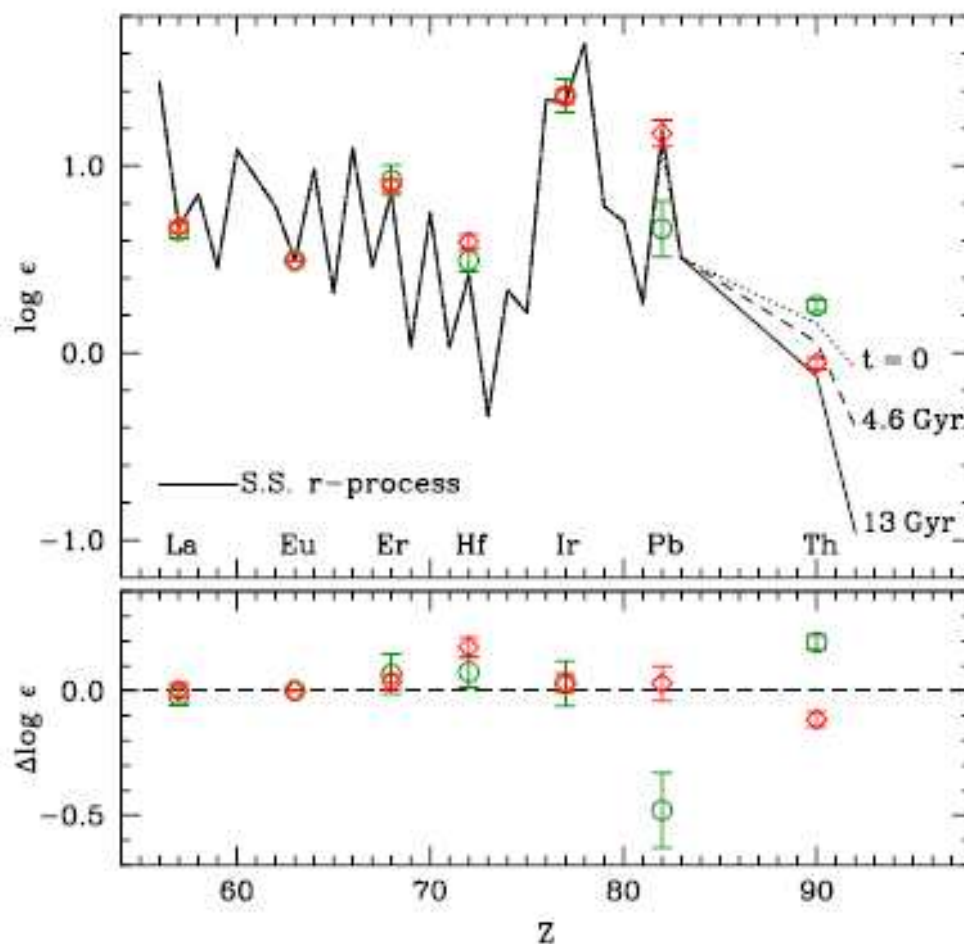


FIG. 8.— Comparison of the mean ratios for stars exhibiting a pure  $r$ -process signature ( $\log \epsilon(\text{La}/\text{Eu}) < +0.25$ ; red diamonds) with the four “actinide boost” stars (green circles). The predicted S.S.  $r$ -process “residual” abundance pattern is shown for reference. The abundances are normalized at Eu. Different decay ages are indicated by the dotted ( $t = 0$  Gyr), dashed ( $t = 4.6$  Gyr), and solid ( $t = 13.0$  Gyr) lines. Any deviations in the abundances of the “actinide boost” stars from the “standard”  $r$ -process stars clearly occur only after the 3<sup>rd</sup>  $r$ -process peak.

Fig. 9.— Demonstration that the “actinide-boost” stars, which have Th/Eu ages of  $\sim 5$  Gyr, are peculiar only for the elements Pb (low) and Th (high) with respect to the  $r$ -process elements in the 3<sup>rd</sup> peak (La, Eu, Er, Hf, and Ir). (Fig. 8 of Roederer, Kratz, Frebel et al, 2009, ApJ, 698, 1963)

### 1.1. Constraints from the *s*-process

My former postdoc Jorge Melendez and I tried to use the metallicity at which nuclei produced in AGN stars can be seen in Galactic halo stars as a time constraint. Its not very precise, but it does work. We used the isotopes of magnesium.  $^{24}\text{Mg}$ , the dominant isotope, is abundantly produced in core-collapse SNII. But the heavy Mg isotopes  $^{25,26}\text{Mg}$ , which are rare, are not part of the main H or He burning chains, and are produced almost exclusively in AGB stars. This too is a difficult measurement. One must use the MgH bands, the isotopic lines are often crowded, blended by other features within the molecular band, and one ends up having to do very detailed spectral syntheses to get a constraint on the age. A minimum spectral resolution of 90,000 is required.

If the AGB contribution is not seen, then an upper limit on the age since the initial burst of star formation is obtained.

This method is not as clean as radioactive decays because a galactic chemical evolution model is required to interpret the data.

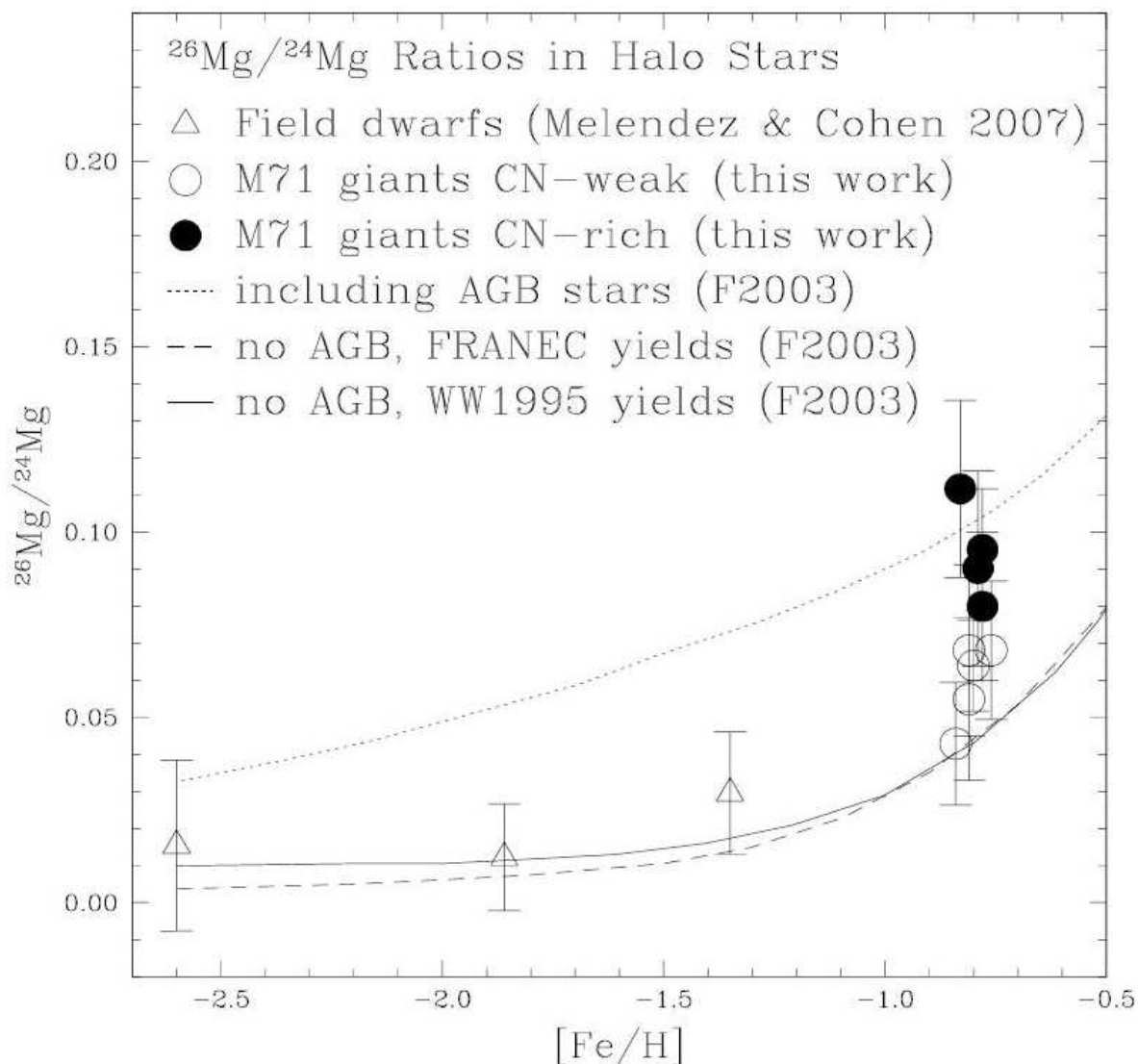


**Fig. 9.** Our  $^{26}\text{Mg}/^{24}\text{Mg}$  ratios in both field dwarfs (triangles; Melendez & Cohen 2007) and M71 giants (circles; this work) as a function of  $[\text{Fe}/\text{H}]$ . Chemical evolution models by Fenner et al. (2003) including (dotted line) and excluding (solid and dashed lines) AGB stars are shown. At the metallicity of M71 ( $[\text{Fe}/\text{H}] = -0.8$ ) the isotopic ratios in the CN-weak stars (open circles) are explained by massive stars, but the CN-strong stars (filled circles) may have been polluted by IM AGB stars.

Fig. 10.— Measurements of the Mg isotopic ratios for halo star compared with the predictions of models of galactic chemical evolution. An upper limit to the timescale for the formation of stars in the halo reaching up to  $[\text{Fe}/\text{H}] \sim -0.8$  dex with no detectable AGB contribution is  $\sim 0.3$  Gyr. (Fig. 10 of Melendez & Cohen, 2009, ApJ, 699, 2017)

## 2. Age Dating from Stellar Evolution

The feature in the CMD usually used for age discrimination is the main sequence turnoff. The problem is that the turnoff is sensitive to heavy elements metallicity and to He content, as well as to age. An evaluation of an age depends on the validity of the full panoply of stellar evolution models, tracks, and isochrones. While ages can be derived for clusters, they are thus quite uncertain due to systematic modeling uncertainties, not to random observational errors.

Another feature of stellar evolution which is somewhat more promising is the population of white dwarfs in clusters. These have no or very little nuclear activity, their luminosity instead comes from the slowly cooling interiors. The luminosity depends on the cooling rate. Thus the distribution with luminosity of a population of white dwarfs such as is found in old globular clusters can be interpreted to yield an age for the system. In particular the detecting the termination at the faint end of the white dwarf sequence is crucial. The theory to treat this is somewhat more straightforward than the MSTO, but still a fairly complex theoretical model is required to interpret the observations. Another disadvantage of this technique is that the white dwarfs are very faint, and the globular clusters are at distances more than 1 kpc.

Brad Hansen has computed the cooling curves for white dwarfs and used this to get an age of 11.5 Gyr (with a claimed accuracy of 5%) for the nearby globular cluster NGC 6397, implying that NGC 6397 formed its stars at  $z = 3.1 \pm 0.6$ , corresponding to an age of  $11.5 \pm 0.5$  Gyr (in the WMAP cosmology). To accomplish this required an enormous effort with HST, a total integration of 50 hours reaching down to mag 27.5 in the F814W filter with the Advanced Camera for Surveys on HST. This cannot be done from the ground because crowding is a serious problem in these rich fields, and a ground-based AO imaging field is too small for studying the white dwarf luminosity distribution. Only a few other



galactic globular clusters are near enough to carry out such an effort even with HST.

In either case, an age cannot be derived for single star through these methods, only for ensembles of stars from a single population with fixed age and metallicity, i.e. a stellar cluster. And in neither case can this be considered a highly accurate age.

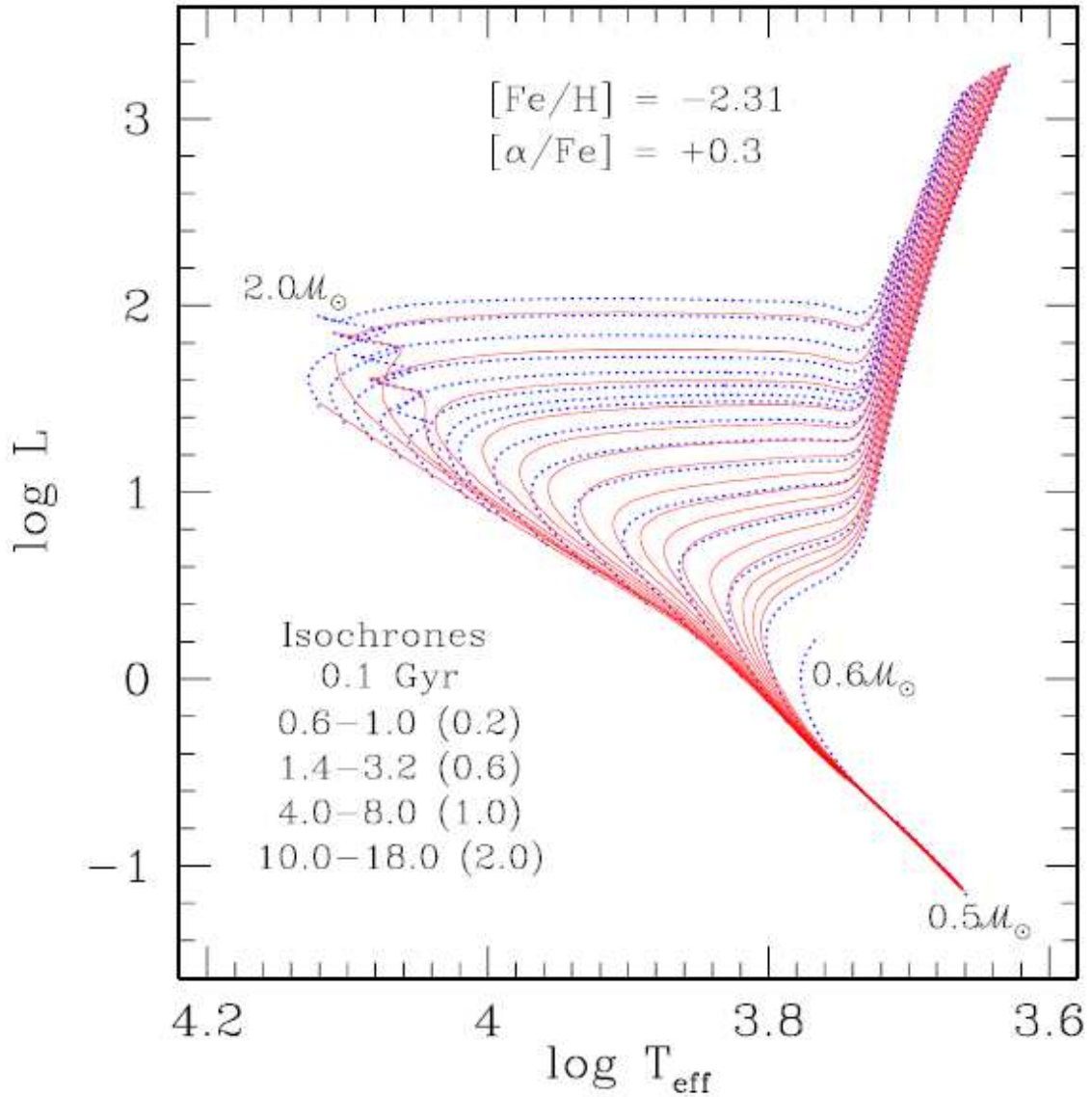


Fig. 9.— The complete grid of evolutionary tracks for the  $[\text{Fe}/\text{H}] = -2.31$ ,  $[\alpha/\text{Fe}] = +0.3$  grid are plotted with the dotted blue lines. The tracks are spaced at  $0.1M_{\odot}$  intervals with an additional track at  $1.44M_{\odot}$ , which is the transitional mass for the development of the blue hook. The isochrones, plotted as solid red lines, span the range of ages from 0.1 to 18.0 Gyr, as indicated.

Fig. 11.— Isochrones for stars of low metal content with ages from 0.1 to 18 Gyr. Note the overlap of all tracks for the lower main sequence where stars of low mass have not yet exhausted their H and the sensitivity of the luminosity and color of main sequence turnoff region to age.

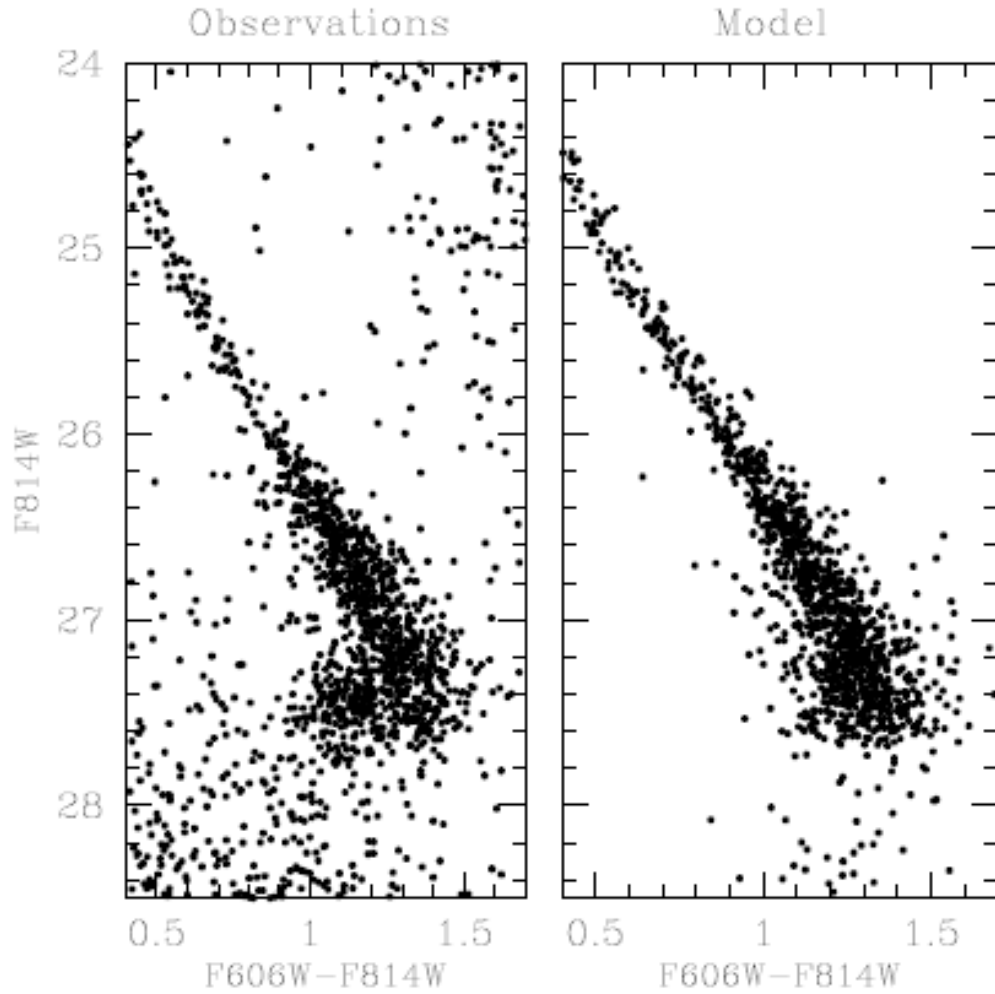


Fig. 11.— The left-hand panel shows the observed cooling sequence, after removal of the majority of background galaxies using `CENXS` cuts. The the right-hand panel shows a monte-carlo realisation of the simulated cooling sequence, adopting the best-fit age of 11.51 Gyr, and modeling the photometric scatter in accordance with the artificial star tests.

Fig. 12.— The white dwarf cooling sequence in the very nearby galactic globular cluster NGC 6397. (Fig. 11 of Hansen, Anderson, Brewer et al, 2007, ApJ, 671, 380)

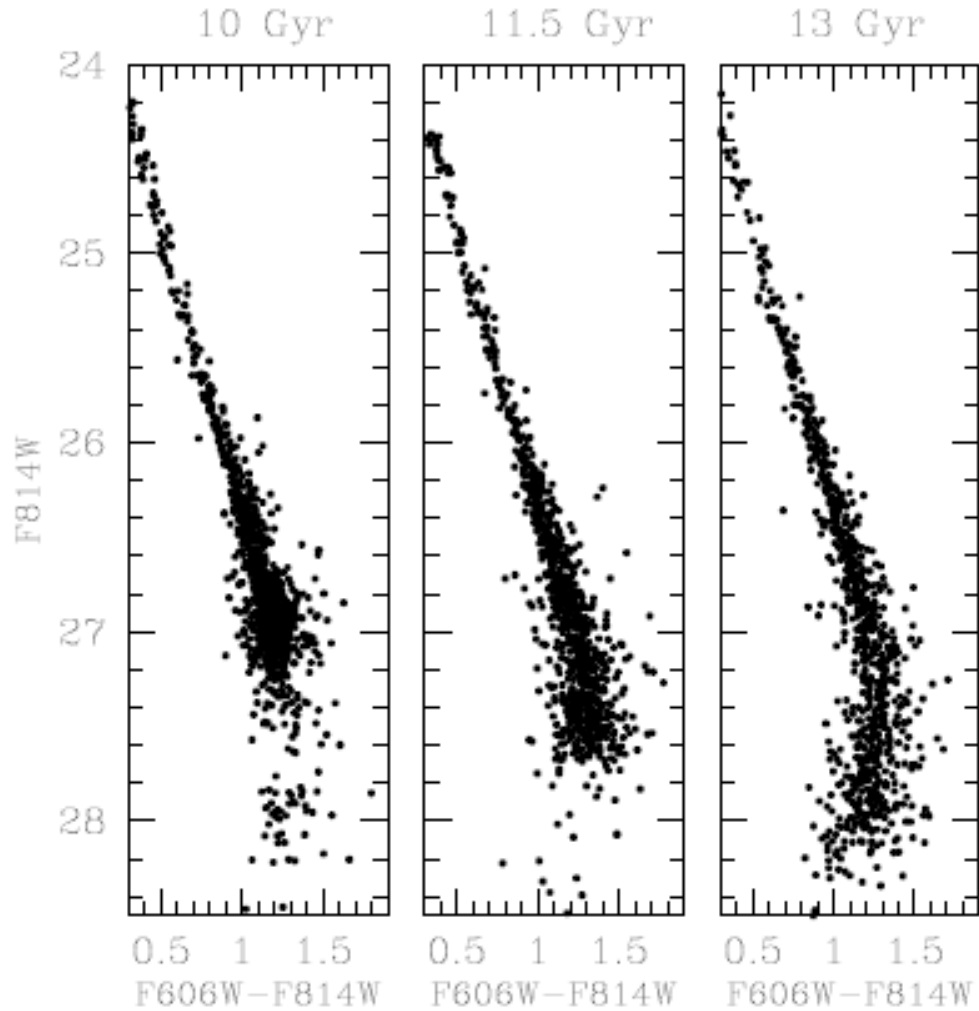


Fig. 23.— The models in all three panels are identical except for the assumed age. The center panel has an age of 11.5 Gyr and corresponds to our best-fit model for NGC 6397. The left hand panel shows a younger population, with age of 10 Gyr, and the right hand panel shows an older one, with age 13 Gyr. It is clear from a simple visual inspection that neither of the side panels are a good match to the observed population seen in Figure [11] or [16].

Fig. 13.— Models with 3 different ages of white dwarf cooling sequence for the very nearby galactic globular cluster NGC 6397. Note that the key age indicator is the faint end of the luminosity distribution of the white dwarf sequence. (Fig. 23 of Hansen, Anderson & Brewer, 2007)

### 3. Suggested Reading

*Explorations of the r-process: comparison between calculations and observations of low-metallicity stars*, Kratz, Farouqi, Pfeiffer, Truran, Sneden, & Cowan, 2007 ApJ, 662, 39

*Probing the Neutron-Capture Nucleosynthesis History of Galactic Matter*, Truran, Cowan, Pilachowski & Sneden, 2002, PASP, 114, 1293 (an extensive review)

*Nucleosynthesis Clocks and the Age of the Galaxy*, Truran, Burles, Cowan & Sneden, conference proceeding, 2002 (see astro-ph/0109526)

*The Extremely Metal-poor, neutron capture-rich star CS 22892-052; A Comprehensive Abundance Analysis*, Sneden, Cowan, Lawler et al, 2003, ApJ, 591, 936. Very metal-poor highly *r*-process enhanced star CS22892-052, 58 elements detected and their abundances established

*The Rise of the AGB in the Galactic Halo: Mg Isotopic Ratios*, 2009, Melendez & Cohen, ApJ, 699, 2017